THE JOURNAL OF PHYSICAL CHEMISTRY C

Article

pubs.acs.org/JPCC

Successive Adsorption of Cations and Anions of Water−1-Butyl-3-methylimidazolium Methylsulfate Binary Mixtures at the Air−Liquid Interface Studied by Sum Frequency Generation Vibrational Spectroscopy and Surface Tension Measurements

Gang-Hua Deng,[†] Xia Li,[‡,§] Shilin Liu,*[,†] Zhen Zhang,[‡] Zhou Lu,[‡] and Yuan Guo*[,‡,§]

[†]Hefei National Laboratory for Physical Sciences at the Microscale, iChEM (Collaborative Innovation Center of Chemistry for Energy Materials), Department of Chemical Physics, University of Science and Technology of China, Hefei 230026, China

[‡]Beijing National Laboratory for Molecular Sciences, State Key Laboratory of Molecular Reaction Dynamics, Institute of Chemistry, Chinese Academy of Sciences, Beijing 100190, China

[§]University of the Chinese Academy of Sciences, Beijing 100049, China

Supporting Information

ABSTRACT: We have investigated the surface behavior of 1-butyl-3-methylimidazolium methylsulfate ([bmim][MS]) aqueous solutions by sum frequency generation vibrational spectroscopy (SFG-VS) and surface tension measurements, including the adsorption of ions and its relationship with surface tension. At very low [bmim][MS] concentrations, SFG-VS data indicate that with increasing mole fraction of [bmim][MS], adsorption of cations at the interface rapidly increases, whereas the surface tension rapidly decreases. When cation adsorption to the surface is close to saturation, the change of the surface tension tends to be gradual. When the mole fraction of [bmim][MS] reaches 0.1, anions begin to adsorb to the interface, leading to the changes of the orientation angle of cations and the aggregation behavior of cations and anions at the interface. The previously reported unusual minimum point in the surface tension curve of [bmim][BF_4] aqueous solution suggested to be caused by successive adsorption of cations and anions was not observed for [bmim][MS] aqueous solution. SFG-VS spectra and the surface tension curve of [bmim][MS] aqueous solution indicate that anion adsorption does not significantly affect the surface tension. These results provide important information about the surface behavior of ionic liquid aqueous solutions and the effect of adsorption of ions on the surface tension.

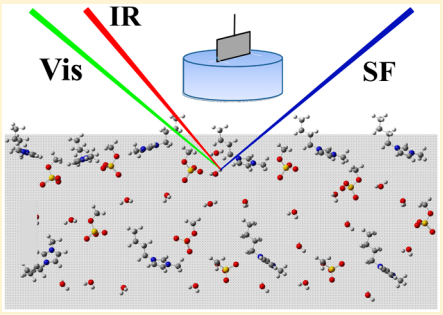

1. INTRODUCTION

Ionic liquids (ILs) are environmentally friendly solvents with unique physicochemical properties. They have been one of the most active scientific research areas in the past decade because of their potential applications in industry. Most of these applications, such as heterogeneous catalysis, electrochemistry, separation, distillation, and gas absorption,[1−9] mainly involve reactions or processes occurring at the surface or interface of the ILs. In many applications of ILs, ILs are in contact with other solvents, such as water, and the investigation of IL−water mixtures has been a topic of much interest.[1,4,10−15] One advantage of ILs in industrial applications is that by selecting the chemical structure of the cation and anion, the physical and chemical properties of the ILs can be tailored for desired industrial applications.[16−24] This requires a deep understanding of the nature of ILs, including their surface properties.

The surface tension is one of the most important surface properties of ILs,[25] and it is directly related to the surface composition and structure of the IL. It is also closely related to intermolecular interactions in the bulk (cohesive energy) and the molecular orientation at the surface,[26,27] which provide a foundation to understand many of the unique properties of ILs. Therefore, investigation of surface phenomena occurring in aqueous solutions of ILs and the surface properties is essential not only for surface science but also for practical applications of ILs.

Investigation of the surface tension of IL−water mixtures has also been of great interest in recent decades. Many of these studies have focused on precise surface tension determination and determining the relationships between surface tension and bulk concentration, and surface tension and the surface structure in IL aqueous solutions.[25,28−46] For example, Bowers et al. investigated the aggregation behavior of [C_4mim][Cl], [C_8mim][Cl], and [C_8mim][I] ILs in aqueous solution using surface tension, conductivity, and small-angle neutron scattering measurements.[29] By varying the bulk concentration, they found that the surface tension of the [C_8mim][Cl] aqueous solution has a pronounced minimum (break point) near the

Received: March 18, 2016
Revised: May 11, 2016
Published: May 16, 2016

DOI: 10.1021/acs.jpcc.6b02841
J. Phys. Chem. C 2016, 120, 12032−12041

critical aggregation concentration (CAC) and then increases with increasing bulk concentration for concentrations greater than the CAC to reach a certain value. Unlike the [C_8mim][Cl] aqueous solution, for the 1-octyl-3-methylimidazolium iodide ([C_8mim][I]) aqueous solution, the surface tension did not show such a minimum. The authors suggested that the observed minimum of the surface tension for the [C_8mim][Cl] aqueous solution may arise from impurities in the IL.[29] At almost the same time, Kim and co-workers used surface tension measurements and surface sum frequency generation vibrational spectroscopy (SFG-VS) to investigate the surface molecular structure of a mixture of 1-butyl-3-methylimidazolium tetrafluoroborate ([bmim][BF_4]) with water.[47] Their main conclusion was that the surface tension of the [bmim][BF_4] aqueous solution exhibits an abnormal low point at a mole fraction of [bmim][BF_4] of about 0.016 when the [bmim][BF_4] mole fraction is increased,[47] which is similar to what was observed in the [C_8mim][Cl] aqueous solution.[29] Considering the SFG-VS spectra at different [bmim][BF_4] concentrations, the authors offered a microscopic explanation for the anomalous minimum in the surface tension curve. They proposed that this unusual behavior of the surface tension may originate from adsorption of BF_4^- anions. For mole fractions less than 0.016, the surface is occupied by [bmim] cations, whereas BF_4^- anions begin to adsorb at the interface for mole fractions greater than 0.016, resulting in a slight increase in the surface tension.

It is still a matter of debate whether successive adsorption of cations and anions in IL aqueous solutions will create an unusual minimum point in the surface tension curve because for a long period of time it was widely accepted that this type of abnormal point is caused by surface-active impurities.[48−50] Indeed, Hoffmann and Russo thoroughly investigated the effect of a variety of conceivable impurities on the surface tension of [bmim][BF_4] aqueous solution.[44] The results showed that the presence of surfactants and oil in the solution could lead to an apparent false minimum in the composition-dependent surface tension.[44] Furthermore, in addition to impurities in IL aqueous solutions, the instability of the IL system may also cause inaccurate measurements. For example, hydrolysis of the BF_4^- anion may result in improper measurement of the surface tension.[51] Other studies have shown that such a surface tension minimum does not exist in [bmim][BF_4] aqueous solutions.[31,41,44,52,53] In summary, although there has been extensive research into IL aqueous solutions, the relationship between surface tension and the concentrations of bulk and interfacial cations and anions is still controversial. Therefore, further research is required to fill in existing gaps in knowledge and resolve any remaining conflicts.

1-Butyl-3-methylimidazolium methylsulfate ([bmim][MS], Figure 1) is an important IL that shows potential as an aerospace lubricant because of its low vapor pressure and good thermal stability.[54] [bmim][MS] and its mixtures with water, alcohol, and other solvents have been extensively studied in recent years.[36,37,55−62] Compared with [bmim][BF_4], [bmim][MS] is a more suitable system to investigate adsorption of ions at the interface because [bmim][BF_4] is prone to hydrolysis in aqueous solution whereas [bmim][MS] is more stable, which can prevent inaccuracies in surface tension measurements caused by system instability. From the viewpoint of accurate determination by SFG-VS, the [bmim][MS] aqueous solution is also more suitable than the [bmim][BF_4] aqueous solution because the vibrational peaks of the BF_4^- anion are around 1000 cm^{-1} where the energy of the infrared (IR) laser is relatively small, resulting in larger errors in SFG-VS measurements. Moreover, the BF_4^- anion is tetrahedral and many of the vibration modes of BF_4^- may not be SFG active, making it difficult for SFG-VS to detect interfacial BF_4^-. For the [bmim][MS] system, the [bmim] cations and [MS] anions both have a methyl group, which can be easily detected by SFG-VS if the ions adsorb to the surface. The [bmim][MS] aqueous solution has not previously been investigated by SFG-VS.

In this work, we use surface tension measurements and sum frequency generation vibrational spectroscopy, a surface-specific spectroscopic technique, to investigate surface adsorption of [bmim] cations and [MS] anions. We also investigate the influence of [bmim] cations and [MS] anions on the surface tension of [bmim][MS] aqueous solution.

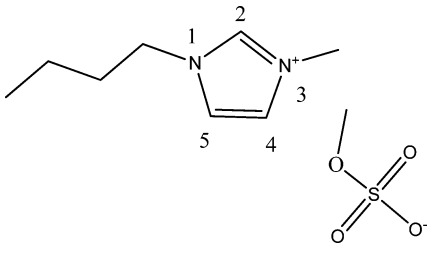

Figure 1. Molecular structure of [bmim][MS].

2. EXPERIMENTAL SECTION

Sum frequency generation vibrational spectroscopy, a second-order nonlinear optical spectroscopic technique, has been widely used to investigate molecular orientations and dynamics at liquid surfaces.[63−65] SFG requires a lack of inversion symmetry, which enables it to probe the top few layers of a surface or interface, where the inversion symmetry is inherently broken. The basic theory and formulation of SFG-VS can be found in the Supporting Information. The SFG spectrometer laser system (EKSPLA, Lithuania) used in the present work has been described in detail elsewhere.[66] Briefly, the 10 Hz and 23 ps SFG spectrometer laser system was arranged in a copropagating configuration. The incident angles of the visible and infrared beams were 45° and 58°, respectively. The visible wavelength was fixed at 532 nm, and the full range of IR tunability was 1000−4000 cm^{-1}. The IR frequency was scanned in 2 cm^{-1} increments. During the experiments, the laser pulse energy was set to 180 μJ for the visible beam and <200 μJ for the IR beam. SFG-VS spectra were recorded with both ssp and ppp polarization combinations. The SFG-VS signals were collected in a reflective geometry, guided into a monochromator (MS 3501; Solar TII, SOL Instruments Ltd., Belarus), and then recorded by an integrated detection system consisting of a high-gain, low-noise photomultiplier (PMT-R585; Hamamatsu) and a dual-channel boxcar averager (Stanford Research Systems). The voltage of the photomultiplier was set to 1300 V for the room-temperature IL measurements. All of the spectra were repeated and averaged several times, and 200 laser pulses per point were accumulated for each scan. The SFG-VS spectral resolution in this work was <6 cm^{-1} for the range of 1000−4000 cm^{-1} and ∼2 cm^{-1} at around 3000 cm^{-1} where the current experiment was carried out. Each spectrum was normalized to the SFG-VS signal of Z-cut quartz. The details of the normalization procedure can be found in the literature.[67]

DOI: 10.1021/acs.jpcc.6b02841
J. Phys. Chem. C 2016, 120, 12032−12041

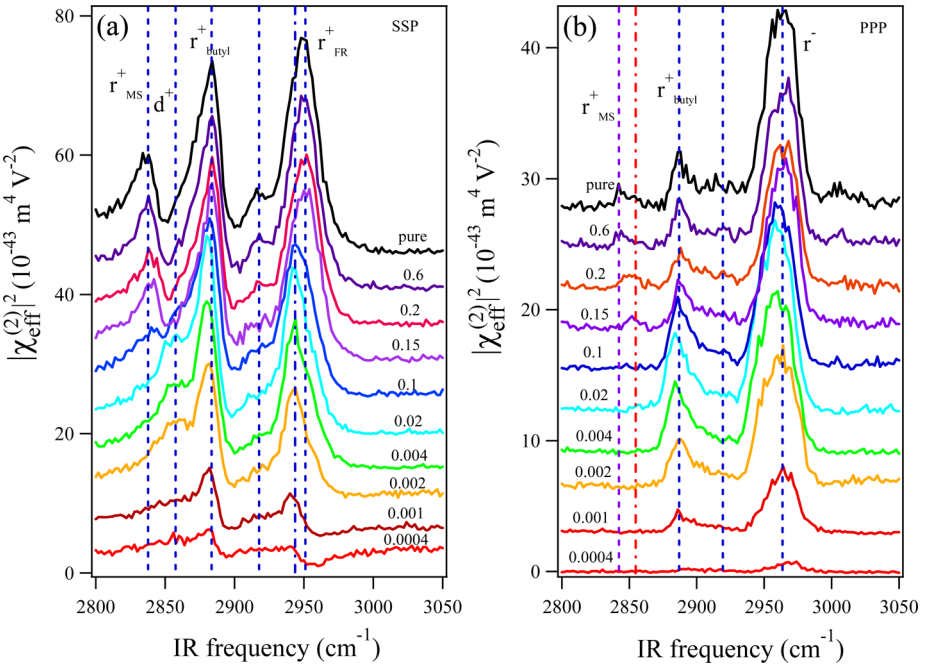

Figure 2. SFG-VS spectra of [bmim][MS] aqueous solutions with different [bmim][MS] mole fractions (0.0004, 0.001, 0.002, 0.004, 0.02, 0.1, 0.15, 0.2, 0.6, and 1): (a) ssp and (b) ppp polarization combinations. The spectra for different [bmim][MS] mole fractions are offset for clarity. The shape and intensity of the SSP spectra significantly change as the mole fraction of [bmim][MS] increases. The ssp spectra show that the peak of the anion (2845 cm^{-1}) appears when the mole fraction of [bmim][MS] reaches 0.1, suggesting that anions adsorb to the surface.

All of the SFG-VS experiments were carried out at controlled room temperature (22.0 ± 0.5 °C) and humidity (40%) in a clean room. The whole SFG-VS setup on the optical table was covered in plastic housing to reduce air flow.

The room-temperature IL [bmim][MS] (>99%) was purchased from Alfa and used without further purification. The water used in the experiment was ultrapure water from standard Millipore treatment (18.2 MΩ cm). The sample was filled in a round Teflon beaker (diameter 5 cm), which was cleaned beforehand by first immersing in Piranha solution for a few hours and then rinsed with ultrapure water from standard Millipore treatment. The surface tension measurements were performed using a processor tensiometer (K100; Kruss, Hamburg, Germany) by the Wilhelmy plate technique. Calibration of the tensiometer was performed by determining the surface tension of ultrapure water.

3. RESULTS AND DISCUSSION

3.1. SFG Spectra of the Air/[bmim][MS] Aqueous Solution Interface. Studies of IL−water mixtures using SFG-VS have been reported before. The Kim group[47] and Baldelli group[68] reported SFG studies of [bmim][BF_4]−water mixture at almost the same time. The SFG-VS spectrum of the pure [bmim][MS] IL also has been previously reported by Baldelli and co-workers,[69−72] who have performed systematic studies of ILs using SFG-VS.[73,74] Especially, they studied the effect of different alkyl chains in both the cation and anion on the surface tension of neat [RMIM][R-OSO_3].[72] However, no SFG-VS spectra of [bmim][MS] aqueous solutions have been reported. To better understand the relationship between the surface tension and the surface structure of [bmim][MS] aqueous solutions, the differences in SFG-VS spectra for different mole fractions of IL [bmim][MS] in aqueous solution were first investigated. Figure 2 shows the C−H stretching region of SFG-VS spectra (ssp and ppp polarization) of air/[bmim][MS] aqueous solution interfaces for 10 different [bmim][MS] mole fractions (0.0004, 0.001, 0.002, 0.004, 0.02, 0.1, 0.15, 0.2, 0.6, and 1). At low mole fractions (0.0004, 0.001, 0.002, 0.004, and 0.02), there are three peaks at around 2860, 2884, and 2945 cm^{-1} in the ssp polarization spectra. According to previous studies,[47,69,75] the peak at 2860 cm^{-1} is the CH_2 symmetric stretching mode (d^+) and the peaks at 2884 and 2945 cm^{-1} are the butyl CH_3 symmetric stretching mode (r^+_{butyl}) and Fermi resonance (r^+_{FR}), respectively.

In the ssp polarization spectra (Figure 2a), when the mole fraction of [bmim][MS] reaches 0.1, a peak appears at 2845 cm^{-1}, which is assigned to the CH_3 symmetric stretching mode (r^+_{MS}) of the [MS] anion,[71,76−78] indicating that the anion starts to adsorb to the surface at a mole fraction of 0.1. The peak at 2860 cm^{-1} gradually disappears when the mole fraction of [bmim][MS] increases to 0.1, indicating that the gauche defect of the butyl chain becomes weak when more cations are adsorbed to the interface. The weak gauche defect indicates that cations are close-packed and well-ordered at high [bmim][MS] mole fractions.[47,68,79] There is also another weak peak at 2915 cm^{-1}, which can be assigned to the CH_2 Fermi resonance (d^+_{FR}) of the butyl chain.[80]

For ppp polarization (Figure 2b), at low [bmim][MS] mole fractions (≤0.02), there are two peaks at around 2884 and 2965 cm^{-1}, which are assigned to CH_3 symmetric stretching and the antisymmetric stretching mode (r^-) of the butyl chain. When the mole fraction increases to 0.15, a peak at 2852 cm^{-1} appears, and then this peak gradually shifts to 2841 cm^{-1} when the [bmim][MS] mole fraction is increased to 1. A more detailed analysis of spectral features that are not directly related to the present discussion is included in the Supporting Information (section S2, Figures S1−S3).

From the peak intensity change of the SFG-VS spectra for different [bmim][MS] mole fractions under ssp and ppp polarization, we can determine the adsorption trend of the

DOI: 10.1021/acs.jpcc.6b02841
J. Phys. Chem. C 2016, 120, 12032−12041

cations and anions of [bmim][MS] in aqueous solution. For mole fractions less than 0.1, with increasing mole fraction of [bmim][MS], the surface is gradually covered by [bmim] cations. When the [bmim][MS] mole fraction reaches 0.1, the CH_3 symmetric stretching peak of the anion appears at 2845 cm^{-1} in the ssp polarization spectrum, which indicates that the anion begins to adsorb to the surface of the solution. In the ppp polarization spectra, the peak of the CH_3 symmetric stretch of the anion starts to appear when the [bmim][MS] mole fraction reaches 0.15. This is because the peak intensity of the CH_3 symmetric stretch of the anion is too weak for 0.1 mole fraction [bmim][MS]. In the ssp polarization spectra, the peak position of Fermi resonance (r^+_{FR}) changes from 2945 to 2952 cm^{-1} with increasing [bmim][MS] mole fraction. The peak intensity also gradually increases and becomes stronger than the symmetric stretching vibration at 2884 cm^{-1}. In general, the intensity of the Fermi resonance peak is weaker than that of the symmetric stretching vibration peak. The ssp polarization spectra in Figure 2a show the opposite trend, which means the Fermi resonance from the CH_3 group of the cation and the anion may both contribute to the peak at around 2950 cm^{-1}.

The r^+_{MS} peak positions in the ppp polarization spectra are different from those in the ssp polarization spectra (Figure 1; can be seen more clearly in Figure S3). The fitting results (Table S3) show that the r^+_{MS} peak position in the ssp polarization spectrum moves from 2845 to 2841 cm^{-1} with increasing [bmim][MS] mole fraction from 0.15 to 1, whereas the r^+_{MS} peak position in the ppp polarization spectrum moves from 2850 to 2841 cm^{-1} (Table S3). The question arises: Why are the r^+_{MS} peak positions of ssp and ppp polarization different? The reason may be that there are anions that have different orientational angles or are subject to different chemical environments at the surface.[81] Similar SFG peak shift between ssp and ppp polarization combinations was also found on vapor/acetonitrile interface by Fourkas and co-workers.[81] They suggested that the methyl and cyanide groups of acetonitrile are sensitive to their environment, such that molecules pointing in opposite directions at an interface can have different transition frequencies. Such shift between peak positions for the same mode can be detected by SFG-VS in ssp and ppp polarization combinations.[82] Our results of [bmim][MS] aqueous solution show the complexity of the surface structure of ILs and their aqueous solutions. More discussion on this issue will be presented in section 3.3

In summary, the SFG-VS spectra for different [bmim][MS] mole fractions indicate that [bmim] cations adsorb to the surface of the [bmim][MS] aqueous solution at low [bmim][MS] mole fractions (<0.1) and that the anion remains in the bulk or near the surface. When the mole fraction reaches 0.1, anions start to adsorb to the surface to balance the net charge of the surface.

3.2. Orientational Angle and Surface Density of Cations and Anions of [bmim][MS]. To quantitatively investigate the orientations of cations and anions at the [bmim][MS] aqueous solution surface, the SFG-VS spectra of different [bmim][MS] mole fractions were fitted, and the results are shown in Tables S1–S3. Table S1 and Table S3 contain the fitting results for mole fractions of 0.0004–0.02 and 0.15–1, respectively. The fitting parameters for mole fraction 0.1 are listed separately in Table S2. The fitting parameters listed in Table S1 were obtained by global fitting of the ssp and ppp spectra for each concentration using the five peaks located at 2862, 2884, 2918, 2944, and 2970 cm^{-1}. For mole fractions of 0.0004 and 0.001, the hydrogen bonded OH stretch (Figure S1) at around 3200 cm^{-1} was also included in the fitting procedure (the fitting parameters of the hydrogen bond peak are not listed in Table S1). According to the above analysis, because of the different r^+_{MS} peak positions in the ssp and ppp spectra, the data for [bmim][MS] mole fractions ≥0.15 cannot be fitted using global fitting. Therefore, only the results of individual fitting are listed in Table S3. In the individual fitting, the five peaks located at 2848, 2884, 2924, 2955, and 2973 cm^{-1} were used. For mole fraction 0.1, as well as the above five peaks, the d^+ peak at 2862 cm^{-1} was also included in the fitting procedure, and the fitting parameters are listed separately in Table S2.

The fitting parameters in Tables S1–S3 indicate that the spectral amplitudes A_q of r^+_{butyl} significantly change with increasing mole fraction. A_q is plotted against the mole fraction of [bmim][MS] in Figure 3.

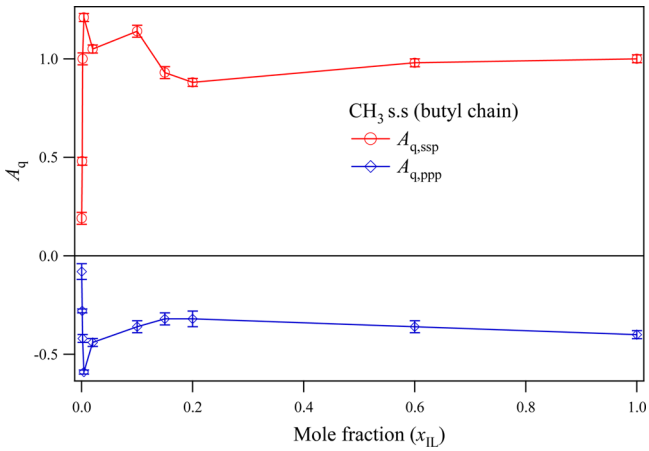

Figure 3. SFG-VS spectral amplitudes of the CH_3 symmetric stretch of the butyl chain plotted against the mole fraction of [bmim][MS]: ssp polarization combinations (red circles, ○) and ppp polarization combinations (blue diamonds, ◊). The solid lines are guides for the eye. The A_q values of the ssp and ppp polarizations rapidly increase with increasing mole fraction of [bmim][MS] for low mole fractions.

Figure 3 reveals that A_q of both ssp and ppp polarization have a similar dependence on the mole fraction of [bmim][MS] except they have the opposite sign. For low [bmim][MS] mole fractions, A_q for both ssp and ppp polarizations rapidly increase with increasing [bmim][MS] mole fraction. When the mole fraction reaches 0.004, A_q reaches a maximum value and then slightly decreases with a further increasing [bmim][MS] mole fraction until it reaches a plateau value. A_q contains information about both the orientation and surface density of interfacial molecules. To determine the surface density for each mole fraction, the orientation angle must first be calculated. As shown by Wang and co-workers, the effective SF susceptibility $\chi^{(2)}_{eff}$ (the basic theory of SFG and detailed formulation about $\chi^{(2)}_{eff}$ can be found in the Supporting Information) can be simplified to the following expression:[64,83]

$$\chi^{(2)}_{eff} = N_s \cdot d \cdot r(\theta) \quad (1)$$

where N_s is the surface density of the probed interfacial species; d is the susceptibility strength factor, which is a constant in a specific experimental configuration for a given molecular system; and $r(\theta)$ is the orientational field functional, which contains all orientational information at a given SFG

DOI: 10.1021/acs.jpcc.6b02841
J. Phys. Chem. C 2016, 120, 12032–12041

Table 1. Concentration (C), Refractive Index ($n(x)$), Orientation Angle (θ), and Surface Density (N_s), of Cations for Different [bmim][MS] Mole Fractions

x_{IL}	0.0004	0.001[a]	0.002	0.004	0.02	0.1	0.15	0.2	0.6	1
C (mol/L)	0.022	0.059	0.11	0.224	1.1	3	3.5	3.7	4.67	4.85
$n(x)$	1.33	1.33	1.33	1.34	1.36	1.42	1.44	1.44	1.47	1.48
θ	32 ± 16	–	32 ± 1.7	23 ± 1.8	34 ± 2.2	48 ± 2.2	46 ± 2.6	44 ± 3.5	45 ± 2.4	42 ± 1.6
N_s	0.25	–	1.32	1.44	1.52	2.48	2.0	1.81	2.16	2.09

[a]For mole fraction of 0.001, no reasonable result can be deduced from the $A_{q,ssp}/A_{q,ppp}$ ratio.

experimental configuration. Equation 1 shows that $\chi^{(2)}_{eff}$ (A_q) is a function of interfacial molecular density N_s and orientation angle θ. Therefore, either a change of N_s or θ can change A_q. It is well-known that the various ratios such as $A_{q,ssp}/A_{q,ppp}$, $A_{q,ssp}/A_{q,sps}$, $A_{q,sps}/A_{q,ppp}$, $A_{q,sps(ss)}/A_{q,sps(as)}$, etc. can be used to calculate the orientation angle in SFG-VS measurements.[63,69,84,85] Therefore, how to choose the ratio to calculate the orientation angle depends on the experimental configuration and the intensity of the SFG-VS signal in the system. Furthermore, previous studies have indicated that $A_{q,ssp}/A_{q,ppp}$ is valid enough for orientation angle analysis.[47,84,86,87] In this report, we first use the ratio $A_{q,ssp}/A_{q,ppp}$ to calculate the orientation angle of the cationic methyl group and then determined N_s of the cation as a function of mole fraction by eq 1. In addition, the interfacial refractive index n' was calculated in terms of the modified Lorentz model of the local field correction.[63] The Raman depolarization ratio for the CH_3 symmetric stretching mode of the [bmim] cation ρ = 0.04 was used to calculate the hyperpolarizability ratio (R) according to Baldelli and Romero.[88] Calculation of n' requires the refractive index n of the bulk aqueous solution, which depends on the bulk concentration of the IL aqueous solution. Detailed calculations of n for different concentrations can be found in the Supporting Information, and the results are listed in Table 1. According to the n values shown in Table 1, the orientation angles of the methyl group of the cation were calculated using the $A_{q,ssp}/A_{q,ppp}$ ratio, and the results are also listed in Table 1. A δ-distribution function of the $-CH_3$ orientational angle was assumed in the calculation.

The orientation angle of the methyl group of the cation as a function of the [bmim][MS] mole fraction of the aqueous solution is shown in Figure 4. At low mole fractions (x_{IL} < 0.1), the methyl group of the butyl chain has a small angle from the surface normal (around 30°). The orientation angle suddenly increases to around 45° at a [bmim][MS] mole fraction of 0.1. With increasing [bmim][MS] mole fraction above 0.1, the orientation angle of the cation methyl group does not greatly change (range 42−48°). At a [bmim][MS] mole fraction of 0.1, anions begin to adsorb to the surface, suggesting that the sudden change of the orientation angle of the cation methyl group may be caused by adsorption of anions.

If θ is known, then N_s can be calculated using eq 1. The relationship between N_s and the bulk [bmim][MS] concentration is plotted in Figure 5. Figure 5a shows that for low mole fractions, as the mole fraction increases, N_s rapidly increases. When the mole fraction reaches 0.1, the surface is saturated with cations (the maximum N_s may be located between 0.02 < x < 0.1 or near 0.1 mole fraction). For increasing mole fraction above 0.1, N_s does not greatly change. Adsorption at the surface

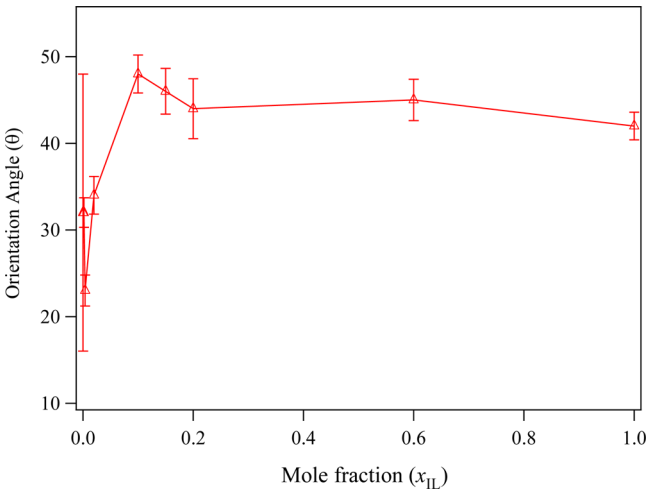

Figure 4. Relationship between the orientation angle of the cation methyl group, θ, and the mole fraction of [bmim][MS].

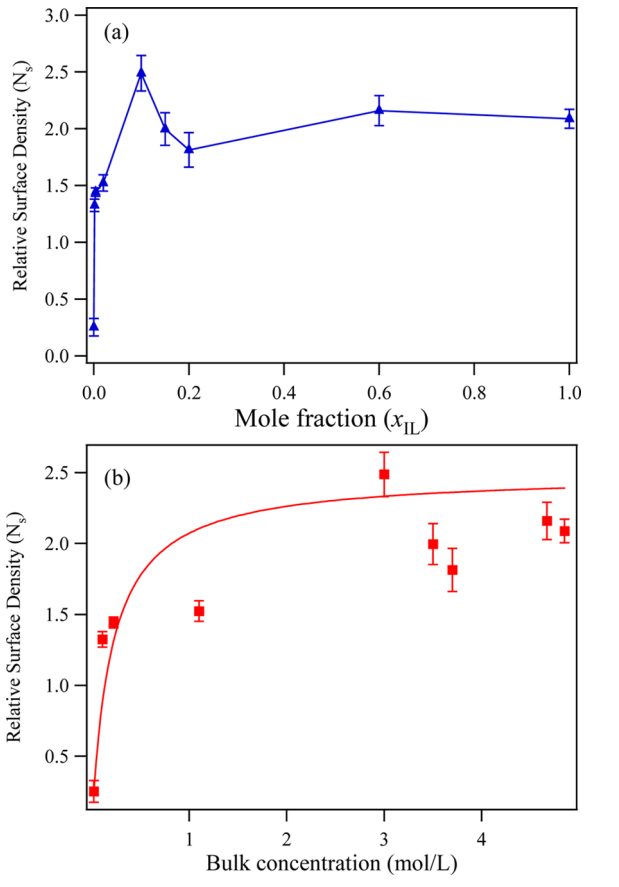

Figure 5. Relationship between relative surface density of the cation N_s and concentration of [bmim][MS]: (a) N_s versus mole fraction and (b) N_s versus bulk concentration (mol/L). The points in panel b are the data, and the solid line is the fitting curve.

DOI: 10.1021/acs.jpcc.6b02841
J. Phys. Chem. C 2016, 120, 12032−12041

of the [bmim][MS] aqueous solution can be described by the classic Langmuirian model, in which the surface density number of the solute can be written as[89]

$$N_s = \frac{N_s^{max} KC}{C_w + KC} \approx \frac{N_s^{max} C}{C + 55.5M \exp(\Delta G_{ads}/RT)} \quad (2)$$

where N_s^{max} is the maximum obtainable surface number density, K the equilibrium constant for occupying a surface site, C the bulk concentration of the solute, and C_w the molar concentration of water, which is approximately 55.5 mol/L in dilute solution. ΔG_{ads} is the Gibbs free energy of adsorption. R (8.314 J mol^{-1} K^{-1}) is the ideal gas constant, and T is the thermodynamic temperature in kelvin. The solid line in Figure 5b is the fitting curve using eq 2, which gives $\Delta G_{ads} = -12.6 \pm 1.1$ kJ·mol^{-1}. This value is comparable to that of some short-chain organic molecules measured by second harmonic generation.[90]

From Figure S3 and Table S3, the peak positions of r^+_{MS} for [bmim][MS] mole fractions of 0.15 and 0.2 for ssp and ppp polarization combinations are different, which may be caused by different types of anion CH_3 groups owing to different molecular orientations or chemical environments. Therefore, the $A_{q,ssp}/A_{q,ppp}$ ratio cannot be used to calculate the anion orientation angle. However, the peak positions of r^+_{MS} for mole fraction 0.6 and pure [bmim][MS] for ssp and ppp polarization combinations are the same, and the calculated orientation angles of the anion methyl group for these two mole fractions are 42° and 34°, respectively. Our result for the orientation angle of the anion methyl group of pure [bmim][MS] is different from the result measured with polarization null angle by Santos et al. (~62°).[71] This may be because the SFG-VS signal of the anion methyl group is weak, especially for ppp polarization (Figure 2b), making the calculated orientation angle not very accurate.

Because we are not able to obtain the orientation angle of the anion methyl group, the surface density cannot be determined from the SFG-VS spectra. However, if we assume that the orientation angle of the anion does not significantly affect the SFG-VS signal, from eq 1, the influence of the orientation angle can be ignored. Using the spectral amplitude $A_{q,ssp}$ instead of the surface density N_s, some qualitative information about the Gibbs energy of adsorption of the anion can still be roughly estimated. Using eq 2, we obtained $\Delta G_{ads} = -9.1 \pm 1.9$ kJ·mol^{-1}.

3.3. Surface Tension of [bmim][MS] Aqueous Solutions. To investigate the relationship between adsorption of cations and anions and the surface tension, the change of the surface tension of [bmim][MS] aqueous solution with [bmim][MS] mole fraction was also measured. The surface tensions of different [bmim][MS] mole fraction aqueous solutions are listed in Table S4 and plotted in Figure 6. Figure 6 shows that for low [bmim][MS] mole fractions, with increasing mole fraction, the surface tension rapidly decreases. When the mole fraction reaches 0.02, the surface tension gradually reaches a plateau. Panda and Paul measured the surface tension of aqueous solutions of [bmim][CH_3SO_3] IL,[91] where the anion [CH_3SO_3]$^-$ is slightly different from [MS] ([CH_3OSO_3]$^-$). Their results were similar to the results shown in Figure 6. However, neither their data nor our data show the anomalous low point observed by Kim and co-workers for [bmim][BF_4][47] and Rogalski and co-workers for [bmim]-[CH_3OSO_3].[55] As suggested in previous studies, for short-chain

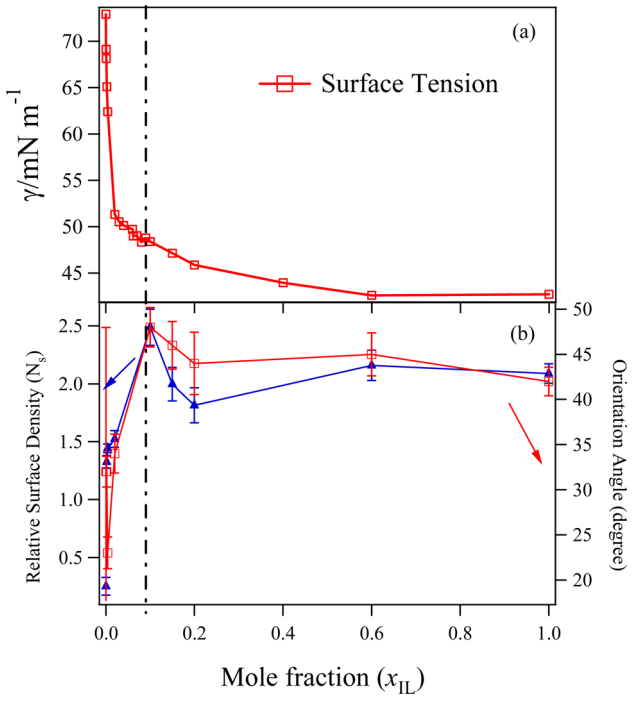

Figure 6. (a) Relationship between surface tension of [bmim][MS] aqueous solution, γ, and mole fraction of [bmim][MS], x_{IL}. (b) Relationships of orientation angle of methyl group of the cation butyl chain, θ, and surface density of [bmim], N_s, with x_{IL}. The black dashed line indicates the concentration where anions start to adsorb to the surface. The rapid decrease of the surface tension of [bmim][MS] aqueous solution is caused by adsorption of cations. No anomalous low point is observed in the data.

ILs composed by cations such as [bmim], the abnormal small valley in the surface tension curve is most likely caused by impurities.[25,44] Naturally, the question may be raised: Are any impurities in our sample which could affect the measurements? We must exclude this factor. The following facts indicate that the sample used in the present work did not contain any impurities affecting the measurements: First, the surface tension curve in Figure 6 did not show a valley. This is indirect but reliable evidence that the sample do not contain any impurities affecting the measurements. The surface tension serves as a standard for detecting impurities in solution. One example given in textbooks is that the surface tension of water will reduce greatly by a very small amount of surfactant or monolayer of organic compound. In addition, the small amount of surfactant or the organic compound can be regarded as impurities for water. It is also true for IL solutions. Hoffmann and Russo thoroughly investigated the effect of a variety of conceivable impurities on the surface tension measurements in aqueous solutions of IL, where they found an unusual minimum in the surface tension measurement caused by the impurities in the sample. For example, the changes of the surface tension are small enough to be neglected by adding acid, alkali, and salt to the aqueous solution, but the presence of surfactants and oil in the solution may lead to an apparent minimum in the composition-dependent surface tension.[44] Our surface tension data shown in Figure 6 indicate that the sample used in our work do not contain any impurities to affect our measurements. Second, the IR spectrum of [bmim][MS] shown in the Supporting Information (Figure S4) also supports

DOI: 10.1021/acs.jpcc.6b02841
J. Phys. Chem. C 2016, 120, 12032−12041

the above conclusion of that the systems do not contain any impurities.

To investigate the relationship between the surface tension and the adsorption of cations and anions at the interface, the surface tension, surface density of cations, and orientation angles of cations and anions are plotted against the mole fraction of [bmim][MS] in Figure 6. The rapidly decreasing region of surface tension and the rapidly increasing region of the surface density of cations are almost in the same mole fraction range (<0.1). This indicates that the decrease of the surface tension of [bmim][MS] aqueous solution is caused by adsorption of cations because anions do not adsorb to the surface at these mole fractions. With further increasing mole fraction of [bmim][MS], the decrease of the surface tension becomes more gradual when the surface tension reaches approximately 50 mN/m. The surface is saturated with cations for a mole fraction of [bmim][MS] of 0.1. Above this mole fraction, anions begin to adsorb to the surface of the solution. However, adsorption of anions does not significantly affect the surface tension. The orientation angle of the cations suddenly changes from around 30° to 40−50° after anions adsorb to the surface (Figure 6b). The concentration at which anion adsorbs to the surface and the sudden change of the tilt angle of cations are in the concentration range where cations and anions aggregate and form micelle-like structures.[25,29,53,92−94] Therefore, it is possible that anions adsorb to the surface and interact with cations as well as aggregating, which may cause the change in the orientation angle of cations. Such segregation of the counterion distribution also occurs in the interfacial region of other IL aqueous solutions.[95] The aggregation process may lead to the existence of different orientations or a variety of aggregation morphologies of anions, resulting in the different peak position of r^{+}_{MS} for ssp and ppp polarization combinations at [bmim][MS] mole fractions of 0.15 and 0.2. At high mole fractions, as the amount of water molecules decreases, aggregation of cations and anions becomes weak and the surface becomes more homogeneous. Therefore, for a [bmim]-[MS] mole fraction of 0.6 and pure [bmim][MS], the peak positions of r^{+}_{MS} for ssp and ppp polarization combinations are almost the same. However, the aggregation behavior and sudden change of the tilt angle do not seem to significantly affect the surface tension. The surface tension of [bmim][MS] aqueous solutions at high mole fractions of [bmim][MS] does not continue to decrease to about 25 mN/m like alcohols and alkanes.[96] This suggests that the interaction between cations and anions at the surface prevents the decrease of the surface tension.

It is worth noting that the number density, N_s, steeply increases from 1.52 to 2.48 as mole fractions increases from 0.02 to 0.1 (Table 1 and Figure 6). Such number density of N_s is increased by a factor of 1.6. However, the surface tension shows a relatively small decrease from 51 to 48 mN/m, which corresponds to the decrease with a factor of only 1.06 times. This result implies that the increment of the number density, N_s, of the cation is not a principal factor inducing the decrease in the surface tension. A possible explanation for this inconsistency is the following: Because surface tension is closely related to intermolecular interactions,[26] different intermolecular effects, such as dipole−dipole interaction, interactions between ions, and hydrophobicity, are able to contribute to the surface tension. The surface-active species can reduce the surface tension because of their weak intermolecular interactions as well as their hydrophobicity,[97] and the inorganic salts increase the surface tension of water because of the electrostatic interactions between ions and water.[98] In the case of our investigation, [bmim][MS] is an organic salt with hydrophobic alkyl groups. Therefore, both the hydrophobicity and the ion−ion and ion−water interactions will affect the surface tension of the solutions. Apparently, for the low concentrations, the rapid decrease of surface tension with increasing mole fraction of [bmin][MS] for low concentrations is caused by the hydrophobicity of the cations. When the concentration reaches a certain value (0.02 mole fraction), more cations adsorb to the surface. The cation−cation and cation−water interactions become strong, and the anions must follow the cations to balance the surface net charge. At this point, the anions tend to stay below the surface, so they have not been observed in the SFG spectra. The decrease of the surface tension caused by the hydrophobicity of cations will be partially compensated by the strong ion−ion and ion−water interactions. This may be the reason that the increment of surface density, N_s, of the cation is still large but the decrease of the surface tension becomes gradual. As the concentration increases to 0.1 mole fraction, anions also adsorb to the surface and the surface layer becomes saturated with both ions. Afterward, adding more IL to the solution does not change the surface tension. Such a physical picture may be able to explain the surface behavior of solutions in the range from 0.02 to 0.1 mole fraction. Further molecular dynamic simulation of [bmin][MS]−water mixtures may be needed to verify such a physical picture.

4. CONCLUSIONS

For [bmim][MS] IL aqueous solutions, we have investigated adsorption of cations and anions to the surface and the relationship between the surface tension and the surface structure of [bmim][MS] by SFG-VS and surface tension measurements. We recorded SFG-VS spectra for different mole fractions of [bmim][MS] in aqueous solution. The results show that for low [bmim][MS] mole fractions, the surface of the [bmim][MS] solution is dominated by cations and that the surface density of cations rapidly increases with increasing mole fraction of [bmim][MS], whereas the surface tension rapidly decreases. This means that the amphiphilic imidazolium cation is surface-active and behaves like a surfactant. As the mole fraction increases to 0.02, the decrease of surface tension becomes gradual. Cations continue to adsorb to the surface, and the surface is saturated with cations for a [bmim][MS] mole fraction of 0.1 (the maximum N_s may be located between $0.02 < x < 0.1$ or near 0.1 mole fraction). Around this mole fraction, anions begin to adsorb to the surface and the orientation angle of the cation methyl group changes from around 30° to 40−50°. The abrupt change in the orientation angle of the cation may be caused by the aggregation of cations and anions. The surface tension curve of [bmim][MS] aqueous solution does not show an unusual minimum point like [bmim][BF_4] aqueous solution, which was attributed to the successive adsorption of cations and anions.[47] The SFG-VS spectra and surface tension curve of [bmim][MS] aqueous solution also suggest that adsorption of anions does not greatly affect the surface tension, which indicates that the surface tension of the [bmim][MS] aqueous solution is dominated by cations and the contribution of anions to it is relatively small. These results shed light on the surface behavior of IL aqueous solutions and provide insight into the surface tension of IL

DOI: 10.1021/acs.jpcc.6b02841
J. Phys. Chem. C 2016, 120, 12032−12041

aqueous solutions as well as other organic salt aqueous solutions.

■ ASSOCIATED CONTENT

Supporting Information

The Supporting Information is available free of charge on the ACS Publications website at DOI: 10.1021/acs.jpcc.6b02841.

Basics of SFG, detailed features of the SFG spectra, and calculation of the refractive index (PDF)

■ AUTHOR INFORMATION

Corresponding Authors

*E-mail: slliu@ustc.edu.cn.

*E-mail: guoyuan@iccas.ac.cn. Tel.: +86 10 62571067. Fax: +86 10 62563167.

Notes

The authors declare no competing financial interest.

■ ACKNOWLEDGMENTS

We thank Prof. Kun Huang and Dr. Chao Zhang for allowing us to perform the surface tension measurements in their laboratory. We thank the Natural Science Foundation of China (NSFC 21227802 and 21073199) and the Ministry of Science and Technology of China (MOST 2013CB834504) for funding.

■ REFERENCES

(1) Castro, G. R.; Knubovets, T. Homogeneous Biocatalysis in Organic Solvents and Water-Organic Mixtures. *Crit. Rev. Biotechnol.* **2003**, *23*, 195−231.

(2) Gutowski, K. E.; Broker, G. A.; Willauer, H. D.; Huddleston, J. G.; Swatloski, R. P.; Holbrey, J. D.; Rogers, R. D. Controlling the Aqueous Miscibility of Ionic Liquids: Aqueous Biphasic Systems of Water-Miscible Ionic Liquids and Water-Structuring Salts for Recycle, Metathesis, and Separations. *J. Am. Chem. Soc.* **2003**, *125*, 6632−6633.

(3) Estager, J.; Holbrey, J. D.; Swadzba-Kwasny, M. Halometallate Ionic Liquids - Revisited. *Chem. Soc. Rev.* **2014**, *43*, 847−886.

(4) Han, X.; Armstrong, D. W. Ionic Liquids in Separations. *Acc. Chem. Res.* **2007**, *40*, 1079−1086.

(5) Rosen, B. A.; Salehi-Khojin, A.; Thorson, M. R.; Zhu, W.; Whipple, D. T.; Kenis, P. J. A.; Masel, R. I. Ionic Liquid-Mediated Selective Conversion of CO_2 to CO at Low Overpotentials. *Science* **2011**, *334*, 643−644.

(6) Vander Hoogerstraete, T.; Wellens, S.; Verachtert, K.; Binnemans, K. Removal of Transition Metals from Rare Earths by Solvent Extraction with an Undiluted Phosphonium Ionic Liquid: Separations Relevant to Rare-Earth Magnet Recycling. *Green Chem.* **2013**, *15*, 919−927.

(7) Scovazzo, P.; Kieft, J.; Finan, D. A.; Koval, C.; DuBois, D.; Noble, R. Gas Separations Using Non-Hexafluorophosphate $[PF_6]^-$ Anion Supported Ionic Liquid Membranes. *J. Membr. Sci.* **2004**, *238*, 57−63.

(8) Scovazzo, P.; Havard, D.; McShea, M.; Mixon, S.; Morgan, D. Long-Term, Continuous Mixed-Gas Dry Fed CO_2/CH_4 and CO_2/N_2 Separation Performance and Selectivities for Room Temperature Ionic Liquid Membranes. *J. Membr. Sci.* **2009**, *327*, 41−48.

(9) Wang, C. M.; Zheng, J. J.; Cui, G. K.; Luo, X. Y.; Guo, Y.; Li, H. R. Highly Efficient SO_2 Capture through Tuning the Interaction between Anion-Functionalized Ionic Liquids and SO_2. *Chem. Commun.* **2013**, *49*, 1166−1168.

(10) Luczak, J.; Hupka, J.; Thoming, J.; Jungnickel, C. Self-Organization of Imidazolium Ionic Liquids in Aqueous Solution. *Colloids Surf., A* **2008**, *329*, 125−133.

(11) Liu, J. F.; Jiang, G.-b.; Liu, J.-f.; Jonsson, J. A. Application of Ionic Liquids in Analytical Chemistry. *TrAC, Trends Anal. Chem.* **2005**, *24*, 20−27.

(12) Kohno, Y.; Ohno, H. Ionic Liquid/Water Mixtures: From Hostility to Conciliation. *Chem. Commun.* **2012**, *48*, 7119−7130.

(13) Romanos, G. E.; Zubeir, L. F.; Likodimos, V.; Falaras, P.; Kroon, M. C.; Iliev, B.; Adamova, G.; Schubert, T. J. S. Enhanced CO_2 Capture in Binary Mixtures of 1-Alkyl-3-Methylimidazolium Tricyanomethanide Ionic Liquids with Water. *J. Phys. Chem. B* **2013**, *117*, 12234−12251.

(14) García Rey, N.; Dlott, D. D. Structural Transition in an Ionic Liquid Controls CO_2 Electrochemical Reduction. *J. Phys. Chem. C* **2015**, *119*, 20892−20899.

(15) de Souza, R. L.; et al. Protic Ionic Liquid as Additive on Lipase Immobilization Using Silica Sol-Gel. *Enzyme Microb. Technol.* **2013**, *52*, 141−150.

(16) Freemantle, M. Designer Solvents: Ionic Liquids May Boost Clean Technology Development. *Chem. Eng. News* **1998**, *76*, 32−37.

(17) Kroon, M. C.; Hartmann, D.; Berkhout, A. Toward a Sustainable Chemical Industry: Cyclic Innovation Applied to Ionic Liquid-Based Technology. *Ind. Eng. Chem. Res.* **2008**, *47*, 8517−8525.

(18) Ohno, H. Functional Design of Ionic Liquids. *Bull. Chem. Soc. Jpn.* **2006**, *79*, 1665−1680.

(19) Short, P. L. Out of the Ivory Tower. *Chem. Eng. News* **2006**, *84*, 15−21.

(20) Olivier-Bourbigou, H.; Magna, L. Ionic Liquids: Perspectives for Organic and Catalytic Reactions. *J. Mol. Catal. A: Chem.* **2002**, *182-183*, 419−437.

(21) Seddon, K. R. Ionic Liquids for Clean Technology. *J. Chem. Technol. Biotechnol.* **1997**, *68*, 351−356.

(22) Reichardt, C. Solvents and Solvent Effects: An Introduction. *Org. Process Res. Dev.* **2007**, *11*, 105−113.

(23) Wilkes, J. S. Properties of Ionic Liquid Solvents for Catalysis. *J. Mol. Catal. A: Chem.* **2004**, *214*, 11−17.

(24) Welton, T. Room-Temperature Ionic Liquids. Solvents for Synthesis and Catalysis. *Chem. Rev.* **1999**, *99*, 2071−2084.

(25) Tariq, M.; Freire, M. G.; Saramago, B.; Coutinho, J. A. P.; Canongia Lopes, J. N.; Rebelo, L. P. N. Surface Tension of Ionic Liquids and Ionic Liquid Solutions. *Chem. Soc. Rev.* **2012**, *41*, 829−868.

(26) Langmuir, I. Forces near the Surfaces of Molecules. *Chem. Rev.* **1930**, *6*, 451−479.

(27) Langmuir, I. Surface Chemistry. Nobel Lecture, December 14, 1932. In *Nobel Lectures, Chemistry 1922-1941*; Elsevier Publishing Company: Amsterdam, 1966

(28) Law, G.; Watson, P. R. Surface Tension Measurements of N-Alkylimidazolium Ionic Liquids. *Langmuir* **2001**, *17*, 6138−6141.

(29) Bowers, J.; Butts, C. P.; Martin, P. J.; Vergara-Gutierrez, M. C.; Heenan, R. K. Aggregation Behavior of Aqueous Solutions of Ionic Liquids. *Langmuir* **2004**, *20*, 2191−2198.

(30) Zang, S. L.; Zhang, Q. G.; Huang, M.; Wang, B.; Yang, H. Z. Studies on the Properties of Ionic Liquid $EMIInCl_4$. *Fluid Phase Equilib.* **2005**, *230*, 192−196.

(31) Liu, W.; Zhao, T.; Zhang, Y.; Wang, H.; Yu, M. The Physical Properties of Aqueous Solutions of the Ionic Liquid $[bmim][BF_4]$. *J. Solution Chem.* **2006**, *35*, 1337−1346.

(32) El Seoud, O. A.; Pires, P. A. R.; Abdel-Moghny, T.; Bastos, E. L. Synthesis and Micellar Properties of Surface-Active Ionic Liquids: 1-Alkyl-3-Methylimidazolium Chlorides. *J. Colloid Interface Sci.* **2007**, *313*, 296−304.

(33) Freire, M. G.; Carvalho, P. J.; Fernandes, A. M.; Marrucho, I. M.; Queimada, A. J.; Coutinho, J. A. P. Surface Tensions of Imidazolium Based Ionic Liquids: Anion, Cation, Temperature and Water Effect. *J. Colloid Interface Sci.* **2007**, *314*, 621−630.

(34) Pereiro, A. B.; Verdia, P.; Tojo, E.; Rodriguez, A. Physical Properties of 1-Butyl-3-Methylimidazolium Methyl Sulfate as a Function of Temperature. *J. Chem. Eng. Data* **2007**, *52*, 377−380.

(35) Carvalho, P. J.; Freire, M. G.; Marrucho, I. M.; Queimada, A. J.; Coutinho, J. A. P. Surface Tensions for the 1-Alkyl-3-Methylimidazolium Bis(Trifluoromethylsulfonyl)Imide Ionic Liquids. *J. Chem. Eng. Data* **2008**, *53*, 1346−1350.

DOI: 10.1021/acs.jpcc.6b02841
J. Phys. Chem. C 2016, 120, 12032−12041

(36) Domanska, U.; Pobudkowska, A.; Rogalski, M. Surface Tension of Binary Mixtures of Imidazolium and Ammonium Based Ionic Liquids with Alcohols, or Water: Cation, Anion Effect. *J. Colloid Interface Sci.* **2008**, *322*, 342−350.
(37) Fernandez, A.; Garcia, J.; Torrecilla, J. S.; Oliet, M.; Rodriguez, F. Volumetric, Transport and Surface Properties of [bmim][$MeSO_4$] and [emim][$EtSO_4$] Ionic Liquids as a Function of Temperature. *J. Chem. Eng. Data* **2008**, *53*, 1518−1522.
(38) Ghatee, M. H.; Zolghadr, A. R. Surface Tension Measurements of Imidazolium-Based Ionic Liquids at Liquid-Vapor Equilibrium. *Fluid Phase Equilib.* **2008**, *263*, 168−175.
(39) Wandschneider, A.; Lehmann, J. K.; Heintz, A. Surface Tension and Density of Pure Ionic Liquids and Some Binary Mixtures with 1-Propanol and 1-Butanol. *J. Chem. Eng. Data* **2008**, *53*, 596−599.
(40) Restolho, J.; Mata, J. L.; Saramago, B. On the Interfacial Behavior of Ionic Liquids: Surface Tensions and Contact Angles. *J. Colloid Interface Sci.* **2009**, *340*, 82−86.
(41) Rilo, E.; Pico, J.; Garcia-Garabal, S.; Varela, L. M.; Cabeza, O. Density and Surface Tension in Binary Mixtures of C_nMIM-BF_4 Ionic Liquids with Water and Ethanol. *Fluid Phase Equilib.* **2009**, *285*, 83−89.
(42) Domanska, U.; Krolikowska, M. Effect of Temperature and Composition on the Surface Tension and Thermodynamic Properties of Binary Mixtures of 1-Butyl-3-Methylimidazolium Thiocyanate with Alcohols. *J. Colloid Interface Sci.* **2010**, *348*, 661−667.
(43) Kolbeck, C.; Lehmann, J.; Lovelock, K. R. J.; Cremer, T.; Paape, N.; Wasserscheid, P.; Froba, A. P.; Maier, F.; Steinruck, H. P. Density and Surface Tension of Ionic Liquids. *J. Phys. Chem. B* **2010**, *114*, 17025−17036.
(44) Russo, J. W.; Hoffmann, M. M. Influence of Typical Impurities on the Surface Tension Measurements of Binary Mixtures of Water and the Ionic Liquids 1-Butyl-3-Methylimidazolium Tetrafluoroborate and Chloride. *J. Chem. Eng. Data* **2010**, *55*, 5900−5905.
(45) Russo, J. W.; Hoffmann, M. M. Measurements of Surface Tension and Chemical Shift on Several Binary Mixtures of Water and Ionic Liquids and Their Comparison for Assessing Aggregation. *J. Chem. Eng. Data* **2011**, *56*, 3703−3710.
(46) Sanchez, L. G.; Espel, J. R.; Onink, F.; Meindersma, G. W.; de Haan, A. B. Density, Viscosity, and Surface Tension of Synthesis Grade Imidazolium, Pyridinium, and Pyrrolidinium Based Room Temperature Ionic Liquids. *J. Chem. Eng. Data* **2009**, *54*, 2803−2812.
(47) Sung, J.; Jeon, Y.; Kim, D.; Iwahashi, T.; Iimori, T.; Seki, K.; Ouchi, Y. Air-Liquid Interface of Ionic Liquid Plus H_2O Binary System Studied by Surface Tension Measurement and Sum-Frequency Generation Spectroscopy. *Chem. Phys. Lett.* **2005**, *406*, 495−500.
(48) Elworthy, P. H.; Mysels, K. J. The Surface Tension of Sodium Dodecylsulfate Solutions and the Phase Separation Model of Micelle Formation. *J. Colloid Interface Sci.* **1966**, *21*, 331−347.
(49) Shaw, D. J.; Costello, B. *Introduction to Colloid and Surface Chemistry*; Butterworth-Heinemann: Oxford, U.K., 1993.
(50) Lin, S.-Y.; Lin, Y.-Y.; Chen, E.-M.; Hsu, C.-T.; Kwan, C.-C. A Study of the Equilibrium Surface Tension and the Critical Micelle Concentration of Mixed Surfactant Solutions. *Langmuir* **1999**, *15*, 4370−4376.
(51) Freire, M. G.; Neves, C.; Marrucho, I. M.; Coutinho, J. A. P.; Fernandes, A. M. Hydrolysis of Tetrafluoroborate and Hexafluorophosphate Counter Ions in Imidazolium-Based Ionic Liquids. *J. Phys. Chem. A* **2010**, *114*, 3744−3749.
(52) Ries, L. A. S.; do Amaral, F. A.; Matos, K.; Martini, E. M. A.; de Souza, M. O.; de Souza, R. F. Evidence of Change in the Molecular Organization of 1-N-Butyl-3-Methylimidazolium Tetrafluoroborate Ionic Liquid Solutions with the Addition of Water. *Polyhedron* **2008**, *27*, 3287−3293.
(53) Liu, W.; Cheng, L.; Zhang, Y.; Wang, H.; Yu, M. The Physical Properties of Aqueous Solution of Room-Temperature Ionic Liquids Based on Imidazolium: Database and Evaluation. *J. Mol. Liq.* **2008**, *140*, 68−72.
(54) Morales, W.; Street, K. W.; Richard, R. M.; Valco, D. J. Tribological Testing and Thermal Analysis of an Alkyl Sulfate Series of Ionic Liquids for Use as Aerospace Lubricants. *Tribol. Trans.* **2012**, *55*, 815−821.
(55) Modaressi, A.; Sifaoui, H.; Mielcarz, M.; Domanska, U.; Rogalski, M. Influence of the Molecular Structure on the Aggregation of Imidazolium Ionic Liquids in Aqueous Solutions. *Colloids Surf., A* **2007**, *302*, 181−185.
(56) Iglesias-Otero, M. A.; Troncoso, J.; Carballo, E.; Romani, L. Densities and Excess Enthalpies for Ionic Liquids Plus Ethanol or Plus Nitromethane. *J. Chem. Eng. Data* **2008**, *53*, 1298−1301.
(57) Calvar, N.; Gonzalez, B.; Dominguez, A.; Macedo, E. A. Osmotic Coefficients of Binary Mixtures of 1-Butyl-3-Methylimidazolium Methylsulfate and 1,3-Dimethylimidazolium Methylsulfate with Alcohols at T = 323.15 K. *J. Chem. Thermodyn.* **2009**, *41*, 617−622.
(58) Calvar, N.; Gonzalez, B.; Gomez, E.; Dominguez, A. Vapor-Liquid Equilibria for the Ternary System Ethanol + Water+1-Butyl-3-Methylimidazolium Methylsulfate and the Corresponding Binary Systems at 101.3 Kpa. *J. Chem. Eng. Data* **2009**, *54*, 1004−1008.
(59) Lin, P. Y.; Soriano, A. N.; Caparanga, A. R.; Li, M. H. Molar Heat Capacity and Electrolytic Conductivity of Aqueous Solutions of [Bmim][$MeSO_4$] and [Bmim][triflate]. *Thermochim. Acta* **2009**, *496*, 105−109.
(60) Singh, T.; Kumar, A. Temperature Dependence of Physical Properties of Imidazolium Based Ionic Liquids: Internal Pressure and Molar Refraction. *J. Solution Chem.* **2009**, *38*, 1043−1053.
(61) Kumar, B.; Singh, T.; Rao, K. S.; Pal, A.; Kumar, A. Thermodynamic and Spectroscopic Studies on Binary Mixtures Ionic Liquids in Ethylene Glycol. *J. Chem. Thermodyn.* **2012**, *44*, 121−127.
(62) Matkowska, D.; Hofman, T. High-Pressure Volumetric Properties of Ionic Liquids: 1-Butyl-3-Methylimidazolium Tetrafluoroborate, [C_4mim][BF_4], 1-Butyl-3-Methylimidazolium Methylsulfate [C_4mim][$MeSO_4$] and 1-Ethyl-3-Methylimidazolium Ethylsulfate, [C_2mim][$EtSO_4$]. *J. Mol. Liq.* **2012**, *165*, 161−167.
(63) Zhuang, X.; Miranda, P. B.; Kim, D.; Shen, Y. R. Mapping Molecular Orientation and Conformation at Interfaces by Surface Nonlinear Optics. *Phys. Rev. B: Condens. Matter Mater. Phys.* **1999**, *59*, 12632−12640.
(64) Wang, H. F.; Gan, W.; Lu, R.; Rao, Y.; Wu, B. H. Quantitative Spectral and Orientational Analysis in Surface Sum Frequency Generation Vibrational Spectroscopy (SFG-VS). *Int. Rev. Phys. Chem.* **2005**, *24*, 191−256.
(65) Arnolds, H.; Bonn, M. Ultrafast Surface Vibrational Dynamics. *Surf. Sci. Rep.* **2010**, *65*, 45−66.
(66) Lu, R.; Gan, W.; Wu, B. H.; Chen, H.; Wang, H. F. Vibrational Polarization Spectroscopy of CH Stretching Modes of the Methylene Group at the Vapor/Liquid Interfaces with Sum Frequency Generation. *J. Phys. Chem. B* **2004**, *108*, 7297−7306.
(67) Gan, W.; Wu, D.; Zhang, Z.; Feng, R. R.; Wang, H. F. Polarization and Experimental Configuration Analyses of Sum Frequency Generation Vibrational Spectra, Structure, and Orientational Motion of the Air/Water Interface. *J. Chem. Phys.* **2006**, *124*, 114705.
(68) Rivera-Rubero, S.; Baldelli, S. Influence of Water on the Surface of the Water-Miscible Ionic Liquid 1-Butyl-3-Methylimidazolium Tetrafluoroborate: A Sum Frequency Generation Analysis. *J. Phys. Chem. B* **2006**, *110*, 15499−15505.
(69) Rivera-Rubero, S.; Baldelli, S. Surface Characterization of 1-Butyl-3-Methylimidazollum Br^-, I^-, PF_6^-, BF_4^-, $(CF_3SO_2)_2N^-$, SCN^-, $CH_3SO_3^-$, $CH_3SO_4^-$, and $(CN)_2N^-$ Ionic Liquids by Sum Frequency Generation. *J. Phys. Chem. B* **2006**, *110*, 4756−4765.
(70) Santos, C. S.; Baldelli, S. Surface Orientation of 1-Methyl-, 1-Ethyl-, and 1-Butyl-3-Methylimidazolium Methyl Sulfate as Probed by Sum-Frequency Generation Vibrational Spectroscopy. *J. Phys. Chem. B* **2007**, *111*, 4715−4723.
(71) Santos, C. S.; Rivera-Rubero, S.; Dibrov, S.; Baldelli, S. Ions at the Surface of a Room-Temperature Ionic Liquid. *J. Phys. Chem. C* **2007**, *111*, 7682−7691.
(72) Santos, C. S.; Baldelli, S. Alkyl Chain Interaction at the Surface of Room Temperature Ionic Liquids: Systematic Variation of Alkyl Chain Length (R = C_1-C_4, C_8) in Both Cation and Anion of

DOI: 10.1021/acs.jpcc.6b02841
J. Phys. Chem. C 2016, 120, 12032−12041

[RMIM][R-OSO_3] by Sum Frequency Generation and Surface Tension. *J. Phys. Chem. B* **2009**, *113*, 923−933.
(73) Baldelli, S. Surface Structure at the Ionic Liquid-Electrified Metal Interface. *Acc. Chem. Res.* **2008**, *41*, 421−431.
(74) Baldelli, S. Interfacial Structure of Room-Temperature Ionic Liquids at the Solid−Liquid Interface as Probed by Sum Frequency Generation Spectroscopy. *J. Phys. Chem. Lett.* **2013**, *4*, 244−252.
(75) Baldelli, S. Influence of Water on the Orientation of Cations at the Surface of a Room-Temperature Ionic Liquid: A Sum Frequency Generation Vibrational Spectroscopic Study. *J. Phys. Chem. B* **2003**, *107*, 6148−6152.
(76) Superfine, R.; Huang, J. Y.; Shen, Y. R. Nonlinear Optical Studies of the Pure Liquid/Vapor Interface: Vibrational Spectra and Polar Ordering. *Phys. Rev. Lett.* **1991**, *66*, 1066−1069.
(77) Ma, G.; Allen, H. C. Surface Studies of Aqueous Methanol Solutions by Vibrational Broad Bandwidth Sum Frequency Generation Spectroscopy. *J. Phys. Chem. B* **2003**, *107*, 6343−6349.
(78) Chen, H.; Gan, W.; Lu, R.; Guo, Y.; Wang, H. F. Determination of Structure and Energetics for Gibbs Surface Adsorption Layers of Binary Liquid Mixture 2. Methanol + Water. *J. Phys. Chem. B* **2005**, *109*, 8064−8075.
(79) Iimori, T.; Iwahashi, T.; Kanai, K.; Seki, K.; Sung, J.; Kim, D.; Hamaguchi, H.-O.; Ouchi, Y. Local Structure at the Air/Liquid Interface of Room-Temperature Ionic Liquids Probed by Infrared-Visible Sum Frequency Generation Vibrational Spectroscopy: 1-Alkyl-3-Methylimidazolium Tetrafluoroborates. *J. Phys. Chem. B* **2007**, *111*, 4860−4866.
(80) Lu, R.; Gan, W.; Wu, B. H.; Zhang, Z.; Guo, Y.; Wang, H. F. C-H Stretching Vibrations of Methyl, Methylene and Methine Groups at the Vapor/Alcohol (n = 1−8) Interfaces. *J. Phys. Chem. B* **2005**, *109*, 14118−14129.
(81) Ding, F.; Hu, Z. H.; Zhong, Q.; Manfred, K.; Gattass, R. R.; Brindza, M. R.; Fourkas, J. T.; Walker, R. A.; Weeks, J. D. Interfacial Organization of Acetonitrile: Simulation and Experiment. *J. Phys. Chem. C* **2010**, *114*, 17651−17659.
(82) Rivera, C. A.; Fourkas, J. T. Reexamining the Interpretation of Vibrational Sum-Frequency Generation Spectra. *Int. Rev. Phys. Chem.* **2011**, *30*, 409−443.
(83) Rao, Y.; Tao, Y. S.; Wang, H. F. Quantitative Analysis of Orientational Order in the Molecular Monolayer by Surface Second Harmonic Generation. *J. Chem. Phys.* **2003**, *119*, 5226−5236.
(84) Bell, G. R.; Bain, C. D.; Ward, R. N. Sum-Frequency Vibrational Spectroscopy of Soluble Surfactants at the Air/Water Interface. *J. Chem. Soc., Faraday Trans.* **1996**, *92*, 515−523.
(85) Zhang, D.; Gutow, J.; Eisenthal, K. B. Vibrational Spectra, Orientations, and Phase Transitions in Long-Chain Amphiphiles at the Air/Water Interface: Probing the Head and Tail Groups by Sum Frequency Generation. *J. Phys. Chem.* **1994**, *98*, 13729−13734.
(86) Velarde, L.; Zhang, X. Y.; Lu, Z.; Joly, A. G.; Wang, Z. M.; Wang, H. F. Communication: Spectroscopic Phase and Lineshapes in High-Resolution Broadband Sum Frequency Vibrational Spectroscopy: Resolving Interfacial Inhomogeneities of "Identical" Molecular Groups. *J. Chem. Phys.* **2011**, *135*, 241102.
(87) Feng, R.-R.; Guo, Y.; Wang, H.-F. Reorientation of the "free OH" Group in the Top-Most Layer of Air/Water Interface of Sodium Fluoride Aqueous Solution Probed with Sum-Frequency Generation Vibrational Spectroscopy. *J. Chem. Phys.* **2014**, *141*, 18C507.
(88) Romero, C.; Baldelli, S. Sum Frequency Generation Study of the Room-Temperature Ionic Liquids/Quartz Interface. *J. Phys. Chem. B* **2006**, *110*, 6213−6223.
(89) Petersen, P. B.; Saykally, R. J. Adsorption of Ions to the Surface of Dilute Electroyte Solutions: The Jones-Ray Effect Revisited. *J. Am. Chem. Soc.* **2005**, *127*, 15446−15452.
(90) Castro, A.; Bhattacharyya, K.; Eisenthal, K. B. Energetics of Adsorption of Neutral and Charged Molecules at the Air/Water Interface by Second Harmonic Generation: Hydrophobic and Solvation Effects. *J. Chem. Phys.* **1991**, *95*, 1310−1315.
(91) Paul, S.; Panda, A. K. Physicochemical Investigations on the Aqueous Solution of an Ionic Liquid, 1-Butyl-3-Methylimidazolium Methanesulfonate, [bmim][MS], in a Concentrated and Dilute Regime. *Colloids Surf., A* **2012**, *404*, 1−11.
(92) Cornellas, A.; Perez, L.; Comelles, F.; Ribosa, I.; Manresa, A.; Garcia, M. T. Self-Aggregation and Antimicrobial Activity of Imidazolium and Pyridinium Based Ionic Liquids in Aqueous Solution. *J. Colloid Interface Sci.* **2011**, *355*, 164−171.
(93) Jungnickel, C.; Luczak, J.; Ranke, J.; Fernandez, J. F.; Muller, A.; Thoming, J. Micelle Formation of Imidazolium Ionic Liquids in Aqueous Solution. *Colloids Surf., A* **2008**, *316*, 278−284.
(94) Li, X. W.; Gao, Y. A.; Liu, J.; Zheng, L. Q.; Chen, B.; Wu, L. Z.; Tung, C. H. Aggregation Behavior of a Chiral Long-Chain Ionic Liquid in Aqueous Solution. *J. Colloid Interface Sci.* **2010**, *343*, 94−101.
(95) Shimamoto, K.; Onohara, A.; Takumi, H.; Watanabe, I.; Tanida, H.; Matsubara, H.; Takiue, T.; Aratono, M. Miscibility and Distribution of Counterions of Imidazolium Ionic Liquid Mixtures at the Air/Water Surface. *Langmuir* **2009**, *25*, 9954−9959.
(96) Dean, J. A. *Lange's Handbook of Chemistry*, 15th. ed.; McGraw-Hill, Inc.: New York, 1999.
(97) Picálek, J.; Minofar, B.; Kolafa, J.; Jungwirth, P. Aqueous Solutions of Ionic Liquids: Study of the Solution/Vapor Interface Using Molecular Dynamics Simulations. *Phys. Chem. Chem. Phys.* **2008**, *10*, 5765−5775.
(98) Bhatt, D.; Newman, J.; Radke, C. Molecular Dynamics Simulations of Surface Tensions of Aqueous Electrolytic Solutions. *J. Phys. Chem. B* **2004**, *108*, 9077−9084.

DOI: 10.1021/acs.jpcc.6b02841
J. Phys. Chem. C 2016, 120, 12032−12041